Molecular Mechanics and Statistical Thermodynamics Studies of Complexes of a Flexible Hemicarcerand with Neutral Guests

Chimin Sheu and K. N. Houk*

Contribution from the Department of Chemistry and Biochemistry, University of California, Los Angeles, Los Angeles, California 90095-1569

Received October 23, 1995. Revised Manuscript Received March 13, 1996[⊗]

Abstract: Computational studies of the structures and conformational properties of hemicarcerand **2**, a model for **1**, studied experimentally by Cram et al., and the complexation and decomplexation of guest molecules by this host have been carried out with MACROMODEL/MM3*. Energy minimizations, molecular dynamics, and statistical perturbation theory calculations were performed. Conformational processes in the intrahemispheric bridges (OCH_2O) of the host molecule have been shown to be important for the passage of guest molecules in and out of the cavity. This transient gate-opening phenomenon has a significant influence on the complexation of bicyclic guests, while smaller aromatic guests can pass in and out without gate-opening. Constrictive binding is crucial for the isolation of hemicarceplexes, since it provides a kinetic barrier which permits isolation of complexes. The 1:1 complexes of hemicarcerand **2** with bicyclic guests and benzene derivatives were found to be energetically favorable by 12−23 kcal/mol in the gas phase. Nevertheless, only the bicyclic guests and some substituted monocyclics form stable complexes. If guests are too large, kinetic barriers prevent complexation. Aromatic guests with disk-like shapes are predicted to form complexes in solution, but to be unstable because of their low decomplexation energy barriers.

Introduction

Synthetic host−guest chemistry holds the dual promise of development of new receptor ligands and model systems for molecular recognition in biological systems. Macrocyclic host molecules, which form thermodynamically stable complexes with neutral or charged guest molecules have been designed to mimic the binding of substrates by enzymes and antibodies, as well as the transport of ions across biological membranes.[1−8]

Cram and co-workers have designed and synthesized a wide variety of cavitand, carcerand, and hemicarcerand host molecules which can complex various guests, such as solvents and small organic molecules, to form caviplexes, carceplexes, and hemicarceplexes.[9−20] These complexes are differentiated by the tenacity with which the guest molecules are bound. Two extreme forms are (1) cavitands, which can form complexes (caviplexes) with organic guests without steric inhibition to either the complexation or the decomplexation processes, and (2) carcerands, which entrap guest molecules within their shells permanently by constrictive binding.

Hemicarcerands are intermediate; they contain portals through which guest molecules can enter or leave the host cavity but with energy barriers high enough to allow isolation and characterization at ordinary temperatures. The binding abilities of hemicarcerands with different guests have been extensively studied by Cram et al.[11,13,14,16−20] Their studies demonstrated several potential applications for these thermodynamically stable complexes.[6,7,21,22]

A principal goal of research in molecular recognition is to understand the interactions between hosts and guests and the factors that control the stability of these complexes. These complexes are held together mainly by noncovalent interactions, such as hydrogen bonding, van der Waals interactions, dipole−dipole interactions, and π-stacking interactions. These forces are much weaker than those of the covalent bonds in organic compounds. An additional mode of binding, constrictive binding, has been invoked by Cram for hemicarceplexes and carceplexes.[6] This mode of binding is defined as the difference between the activation energy for dissociation and the thermodynamic binding energy. It represents the physical barrier which prevents escape by the guest.

With the help of CPK (Corey−Pauling−Koltun) molecular models, the complementarity between host and guest molecules

[⊗] Abstract published in *Advance ACS Abstracts,* May 1, 1996.

(1) Cram, D. J.; Cram, J. M. *Science (Washington, DC)* **1974**, *183*, 803.
(2) Cram, D. J. In *Applications of Biochemical Systems in Organic Chemistry*; Jones, J. B., Sih, C. J., Perlman, D., Eds.; Wiley, New York, 1976; pp 815−873.
(3) Cram, D. J. *Acc. Chem. Res.* **1978**, *11*, 8.
(4) *Host Guest Complex Chemistry I*; Vögtle, F., Ed.; Springer: Berlin, 1981; Vol. 98.
(5) *Host Guest Complex Chemistry II*; Vögtle, F., Ed.; Springer: Berlin, 1982; Vol. 101.
(6) Cram, D. J. *Angew. Chem., Int. Ed. Engl.* **1988**, *27*, 1009−1112.
(7) Cram, D. J. *Nature* **1992**, *356*, 29−36.
(8) Cram, D. J.; Cram, J. M. *Container Molecules and Their Guests*; Royal Society of Chemistry: Cambridge, England, 1994.
(9) Tunstad, L. M.; Tucker, J. A.; Dalcanale, E.; Weiser, J.; Bryant, J. A.; Sherman, J. C.; Helgeson, R. C.; Knobler, C. B.; Cram, D. J. *J. Org. Chem.* **1989**, *54*, 1305−1312.
(10) Tucker, J. A.; Knobler, C. B.; Trueblood, K. N.; Cram, D. J. *J. Am. Chem. Soc.* **1989**, *111*, 3688−3699.
(11) Tanner, M. E.; Knobler, C. B.; Cram, D. J. *J. Am. Chem. Soc.* **1990**, *112*, 1659−1660.
(12) Bryant, J. A.; Blanda, M. T.; Vincenti, M.; Cram, D. J. *J. Chem. Soc., Chem. Commun.* **1990**, 1403−1405.
(13) Quan, M. L. C.; Cram, D. J. *J. Am. Chem. Soc.* **1991**, *113*, 2754−2755.
(14) Quan, M. L. C.; Knobler, C. B.; Cram, D. J. *J. Chem. Soc., Chem. Commun.* **1991**, 660−662.
(15) Moran, J. R.; Ericson, J. L.; Dalcanale, E.; Bryant, J. A.; Knobler, C. B.; Cram, D. J. *J. Am. Chem. Soc.* **1991**, *113*, 5707−5714.
(16) Cram, D. J.; Tanner, M. E.; Knobler, C. B. *J. Am. Chem. Soc.* **1991**, *113*, 7717−7727.
(17) Choi, H.-J.; Buhring, D.; Quan, M. L. C.; Knobler, C. B.; Cram, D. J. *J. Chem. Soc., Chem. Commun.* **1992**, 1733−1735.
(18) Cram, D. J.; Jaeger, R.; Deshayes, K. *J. Am. Chem. Soc.* **1993**, *115*, 10111−10116.
(19) Robbins, T. A.; Knobler, C. B.; Bellew, D. R.; Cram, D. J. *J. Am. Chem. Soc.* **1994**, *116*, 111−122.
(20) Cram, D. J.; Blanda, M. T.; Paek, K.; Knobler, C. B. *J. Am. Chem. Soc.* **1992**, *114*, 7765−7773.
(21) Cram, D. J.; Tanner, M. E.; Thomas, R. *Angew. Chem., Int. Ed. Engl.* **1991**, *30*, 1024−1027.
(22) Robbins, T. A.; Cram, D. J. *J. Am. Chem. Soc.* **1993**, *115*, 12199.

S0002-7863(95)03542-6 CCC: $12.00

Chart 1

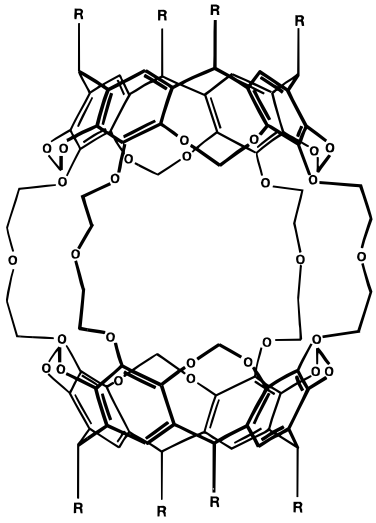

1. R = $PhCH_2CH_2$
2. R = H

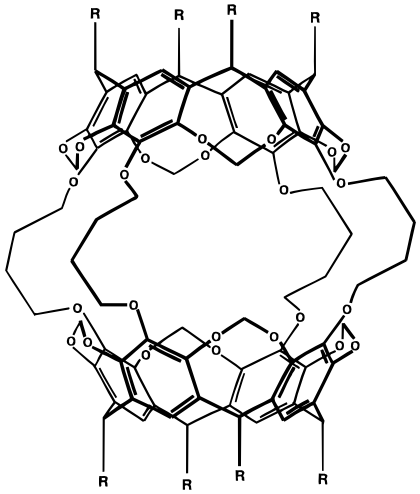

3. R = $PhCH_2CH_2$
4. R = H

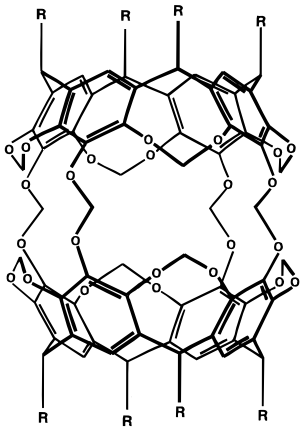

5. R = $PhCH_2CH_2$
6. R = H

was fruitfully examined by Cram and co-workers. However, quantitative information about the origins of selectivity is not available by this method. We have undertaken a research program to develop computational methods to understand the structures, stabilities, and dynamics of carceplexes and hemicarceplexes in solution. The general goals of this investigation are twofold: (1) can computational methods reproduce the experimental trends of interest and (2) can we provide an explanation of why some guests give isolable complexes, while other similar molecules do not form isolable complexes? In previous papers, we reported that Cram's carcerands and hemicarcerands have "gates", functionalities which can "open" and "close" by conformational processes. These conformational processes may be the rate-determining steps in passage of guests in and out of the host cavity.[23] In this paper, we study a different hemicarceplex and explore the energetics of binding and decomplexation.

The molecules **1**, **3**, and **5**, synthesized by Cram and co-workers, each display different behavior. Hemicarcerand **1** forms isolable complexes with a variety of small molecules, including *trans*-1,2-dibromocyclohexane and bicyclic molecules such as norbornane. These hemicarceplexes are formed by equilibration experiments in solution. Larger bicyclics such as camphor do not form complexes. More surprisingly, a large number of simple aromatics, from benzene through dimethoxybenzene and 3-methylcatechol, also do not form stable complexes.[24]

Hemicarcerand **3** has one fewer oxygen atom in each linker. In contrast to **1**, compound **3** forms stable complexes with most simple aromatic compounds.[19] Here the cavity is somewhat smaller, and either attractive interactions in the cavity, or constrictive binding, hold the guests inside. The carcerand **5**, and the simpler derivative, **6**, were first made in the Cram group[25,26] and have been studied extensively by Sherman and co-workers.[27−29] Carceplexes containing various aromatic guests and a variety of solvent molecules can be formed during synthesis. Since **5** has much smaller portals than **1** or **3**, the incarceration of guests occurs only during synthesis, and the guests do not escape.

In this paper, we report studies of the complexation of guest molecules by hemicarcerand **2**, a model for the more highly substituted **1**. Studies of the complexes of **3** and **5** are in progress and will be reported elsewhere.

Background

Hemicarcerand **1** is composed of two rigid tetraaryl bowl-like units joined with four $O(CH_2)_2O(CH_2)_2O$ units as equatorial spacers. The pendant $C_6H_5CH_2CH_2$ groups were used experimentally to produce better solubility and crystallization properties. For computational simplification, we replaced these phenethyl groups with hydrogen atoms. The model **2** was used in all computational studies.

Cram and co-workers surveyed a large number of small molecules to determine which would form stable complexes. The complexation experiments were carried out as follows: 10−20 mg of hemicarcerand **1** and 100−200 fold excess of guest, either neat or in 0.2−1.0 mL of *N*,*N*-dimethylacetamide (DMA) or diphenyl ether (Ph_2O) as co-solvent, were placed in a sealed vial. The reaction mixture was refluxed at temperatures of 70−190 °C for several days. The mixture was then poured into 50 mL of hexane or methanol, and the resulting precipitate was filtered and purified by preparative silica gel chromatography with 5% acetone in chloroform as eluent.[24] In order for a complex to be isolated under such conditions, the guest must be able to enter the cavity, and the complex must be stable to chromatography.

Hemicarcerand **1** forms complexes with various guests, such as *trans*-1,2-dibromocyclohexane, bicyclics, and some trisubstituted benzene derivatives. These are shown in Chart 2. Other guests, such as 2,3-dichlorobutane, camphor, and a large number of simple aromatics shown in Chart 3 either fail to complex or

(23) Nakamura, K.; Houk, K. N. *J. Am. Chem. Soc.* **1995**, *117*, 1853−1854. Houk, K. N.; Nakamura, K.; Sheu, C.; Keating, A. E. *Science* **1996**, *273*, 627.

(24) Byun, Y.-S.; Vadhat, O.; Blanda, M. T.; Knobler, C. B.; Cram, D. J. *J. Chem. Soc., Chem. Commun* **1995**, 1825−1827.

(25) Sherman, J. C.; Cram, D. J. *J. Am. Chem. Soc.* **1989**, *111*, 4527−4528.

(26) Sherman, J. C.; Knobler, C. B.; Cram, D. J. *J. Am. Chem. Soc.* **1991**, *113*, 2194−2204.

(27) Chapman, R. G.; Chopra, N.; Cochien, E. D.; Sherman, J. C. *J. Am. Chem. Soc.* **1994**, *116*, 369−370.

(28) Fraser, J. R.; Borecka, B.; Trotter, J.; Sherman, J. C. *J. Org. Soc.* **1995**, *60*, 1207−1213.

(29) Chopra, N.; Sherman, J. C. *Supramolecular Chemistry* **1995**, *5*, 31−37.

Chart 2. Guests which Form Isolable Complexes with Hemicarcerand 1

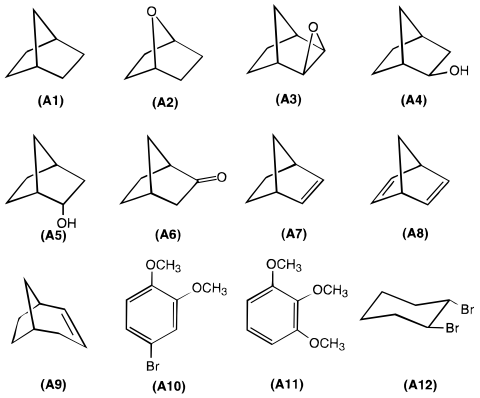

Chart 3. Guests which Do Not Form Isolable Complexes with Hemicarcerand 1

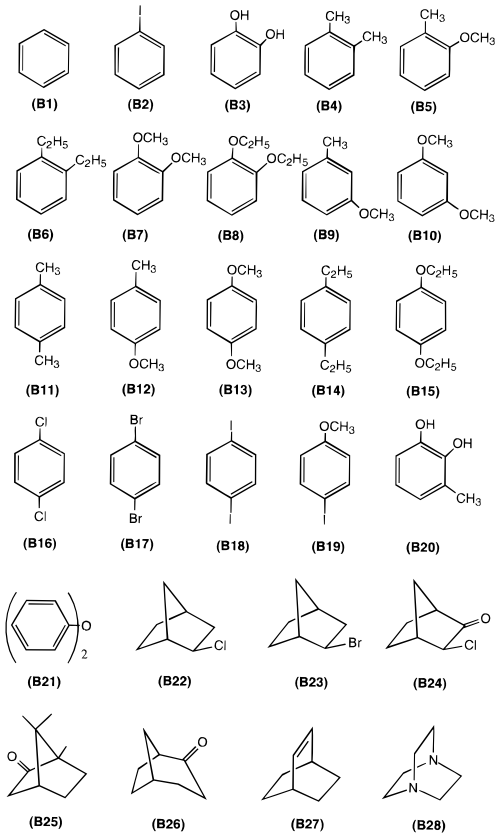

do not remain trapped in the host upon attempted isolation.[24] Thus, hemicarcerand **1** displays a high degree of shape and size selectivity.

In order to understand this shape and size selectivity, molecular mechanics and statistical thermodynamics studies of the formation and stability of 1:1 complexes of hemicarcerand **2** with both bicyclic and aromatic guests were performed.

Computational Methods

Force field calculations were carried out using the MM3* force field in the MACROMODEL program.[30] In other work, we have explored the use of various parameterizations of MM2*, MM3*, and AMBER* force fields for the study of complexation phenomena. There are significant differences in these three force fields which will be discussed in due course.[31] In general, trends in relative complex energies are similar with all methods, but barriers to conformational processes and decomplexation are different with different force fields.

Conformations of the hemicarcerand **2** were explored with a Monte Carlo (MC) search by varying the torsional angles in the four interhemispheric bridges. The starting geometry for MC search was created with the MACROMODEL program. The total MC steps are 5000, each MC step begins with the starting geometry of the least used structure of previous MC steps. Starting geometries on the hemicarcerand-neutral guest complexes were obtained manually by docking the neutral guest inside the cavity of the hemicarcerand in various orientations. These were energy minimized with the MM3* force field. The lowest energy conformer of each carceplex was then used as the starting geometry in an optimization using the simulated annealing method. The cooling process is linear and continuous from 400 to 50 K over a 200 ps molecular dynamics simulation.

Molecular dynamics simulations were also carried out with the MACROMODEL program to evaluate the average enthalpies upon complexation of **2** with bicyclic guests **A1** and **B25**. The simulation temperature was set at 373 K (experimental temperature), and the time step was 0.5 fs. All structures were equilibrated at 373 K for 5 ps before each molecular dynamics run. The total simulation times for guest, host, and complex are 20, 100, and 200 ps, respectively, which were found to be sufficient for energy convergence.

Results and Discussion

Conformational Analysis of 2. Cram gave names to the regions of carcerands; using a global analogy, he named them as polar, temperate, and equatorial regions. Although the two polar tetraaryl bowls are relatively rigid, both the intra- and interhemispheric linkers are very flexible. The possible geometries of **2** were explored by a Monte Carlo conformational search with MM3* force field optimizations. The Monte Carlo conformational search generated hundreds of different conformers. Among them, three highly symmetrical conformers were located. These are shown in Figure 1. The energetics of the different conformations of four interhemispherical bridges connecting the two bowls were also examined.

Structure **2a** is the global minimum; it has D_{2h} symmetry. The two polar bowls are perfectly eclipsed with a C_4 polar axis, but the bridges are related only by a C_2 axis. In this geometry, the unshared electron pairs of eight oxygen atoms on the intrahemispheric bridges (Ar$\underline{O}CH_2\underline{O}$Ar) of the northern and southern bowls are facing outward away from the cavity, and the central methylene groups (ArO$\underline{CH_2}$OAr) are facing inward toward the cavity to form a chair-like eight-membered ring. The orientations of these intrahemispheric bridges have an influence on the size and shape of the side portals, as will be discussed in more detail later.

In addition, the unshared electron pairs of the eight oxygen atoms (two for each bridge) on the rims of the four interhemispheric linkers ($\underline{O}CH_2CH_2OCH_2CH_2\underline{O}$) all face into the cavity, and the bonds from these oxygens to the methylene groups (O$\underline{CH_2}$CH$_2$OCH$_2$$\underline{CH_2}$O) are facing outward away from the cavity. Each of the four benzene rings of the northern and southern polar caps has the unshared electron pairs of three adjacent oxygens with an out−in−out orientation (Figure 2a). The portals and cavity of this structure are longer in the equatorial dimension and shorter in the polar dimension. The average vertical distance between two intrahemispheric linkage carbon atoms (O$\underline{CH_2}$O) in northern and southern bowls is approximately 5.6 Å, and the average equatorial dimension is

(30) Mohamadi, F.; Richards, N. G. J.; Guida, W. C.; Liskamp, R.; Caufield, C.; Chang, G.; Hendrickson, T.; Still, W. C. *J. Comput. Chem.* **1990**, *11*, 440.

(31) Houk, K. N.; Nakamura, K.; Sheu, C.; Constable, A. E. Submitted for publication.

(32) Byun, Y.-S.; Vadhat, O.; Blanda, M. T.; Knobler, C. B.; Cram, D. J. Unpublished results.

(33) Nash, L. K. *J. Chem. Educ.* **1984**, *61*, 981−984.

(34) Davies, M. In *CRC Handbook of Chemistry and Physics*, 66th ed.; Weast, R. C., Astle, M. J., Beyer, W. H., Eds.; CRC Press: Boca Raton, FL, 1986; pp C664-C665, and reference therein.

(35) Sheu, C.; Houk, K. N. Unpublished results.

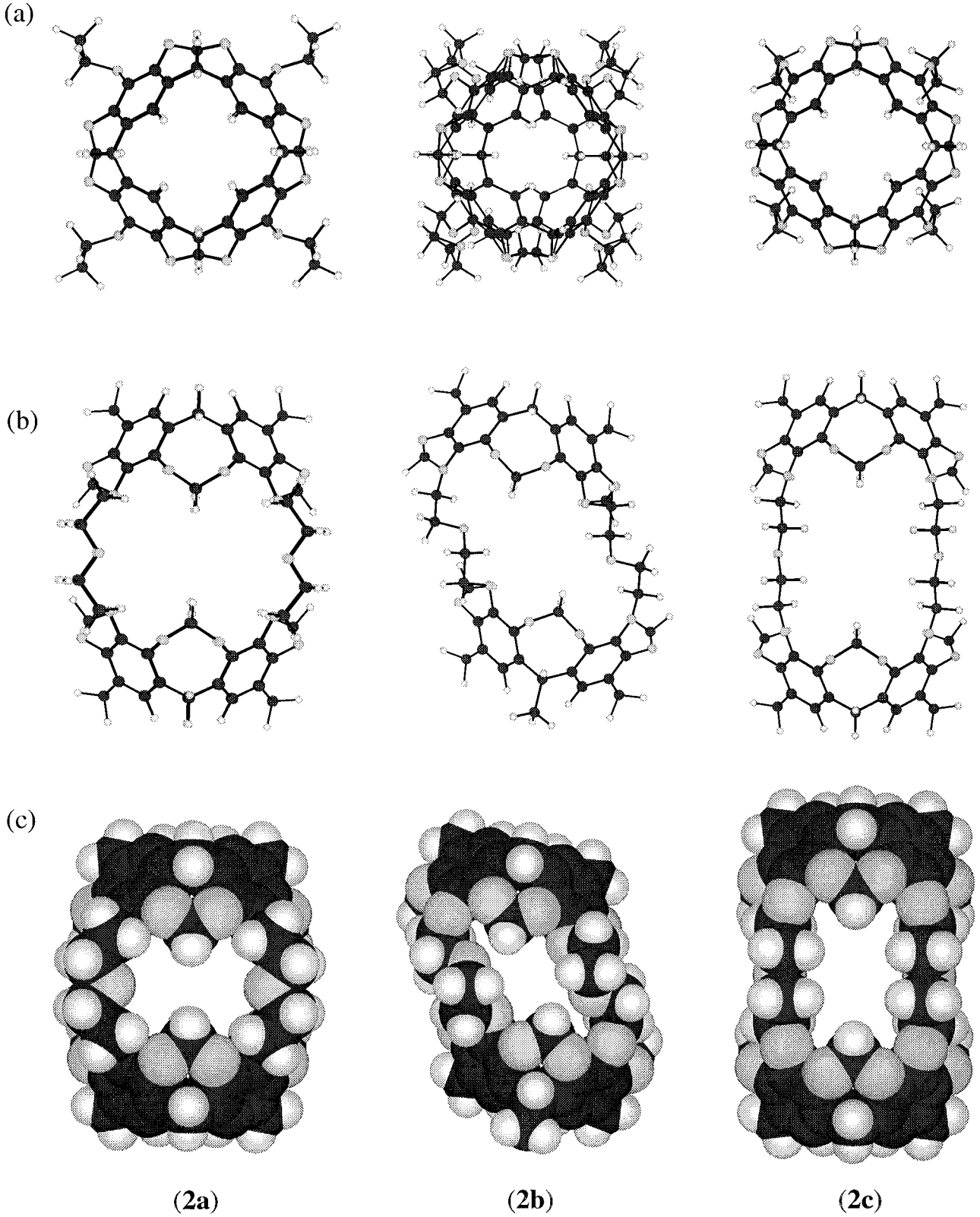

Figure 1. Three low energy conformers of hemicarcerand **2** (**2a**−**c**) optimized by molecular mechanics method (MM3*): (a) top views, (b) side views, and (c) space-filling models.

8.8 Å between two central oxygen atoms ($OCH_2CH_2\underline{O}CH_2$-$CH_2O$) of two adjacent interhemispheric linkages.

Structure **2b** was found to be very similar to the X-ray structures of hemicarcerand **2** with $2CH_2Cl_2$ and $2H_2O$ molecules[24] and of hemicarcerand **2** with six water molecules[32] inside the cavity (Figure 3). Here the two bowls of the host molecule are displaced horizontally to form a rhomboidal cavity. Conformer **2b** has C_{2h} symmetry and is calculated to be 7.6 kcal/mol higher in energy than **2a**. As with **2a**, **2b** has the chair orientations for its intrahemispheric linkages ($ArOCH_2OAr$). The CH_2 groups nearest the northern and southern bowls ($O\underline{CH_2}$-$CH_2OCH_2\underline{CH_2}O$) are arranged alternately facing outward and inward (see Figure 2b). This is the arrangement found in the X-ray structure (Figure 3).

Conformer **2c** is calculated to be 9.2 kcal/mol higher in energy than **2a**. It has the two polar bowls perfectly eclipsed and D_{2h} symmetry. The main difference between **2a** and **2c** lies in the orientations of CH_2 groups attached to the eight oxygen atoms

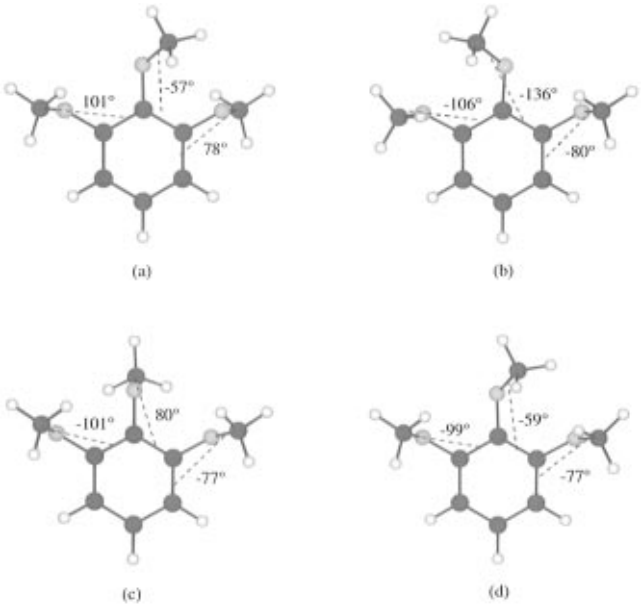

Figure 2. Representative orientations of groups attached to the three adjacent oxygen atoms on the benzene rings of the polar cap in (a) **2a**, (b) and (c) **2b**, and (d) **2c**. Dihedral angles are shown for each.

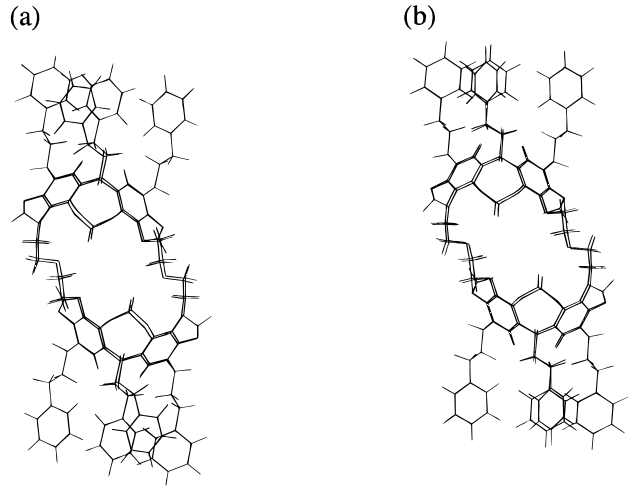

Figure 3. (a) X-ray structure of hemicarcerand (**1**). (b) X-ray structure of hemicarcerand (**1**) after minimization with MM3* force field. (Six water molecules inside the cavity have been omitted for clarity).

($O\underline{CH_2}CH_2OCH_2\underline{CH_2}O$) on the interhemispheric linkages. In contrast to **2a**, **2c** has all of these CH_2 groups facing inward. This arrangement places all the unshared electron pairs from three adjacent oxygen atoms on the benzene rings of polar bowls pointing outward (Figure 2d). In this geometry, the portals of **2c** are longer in polar dimension (8.0 Å) than the equatorial dimension (6.7 Å).

In addition to these symmetric conformers, there are hundreds of other conformations composed of approximately gauche and anti torsion angles in the interhemispheric linkages, but having approximately the three torsional arrangements of the aryl-O dihedral angles as **2a**, **b**, or **c**. The energetic effects caused by rotating around single bonds joining the underlined atoms on the interhemispheric bridges ($O\underline{CH_2CH_2OCH_2CH_2}O$) of the host molecule have also been examined. The results show that changing these bridge conformations has little effect on the energy if the host molecule has a geometry similar to **2a** or **2c**. For example, varying one or two bridges in **2c** leads to only an energy increase of 0.1 kcal/mol (Figure 4) and with an average increase of only 0.2 kcal/mol for other conformers. However, the conformations of these bridges have much larger energetic effects if the two bowls of the host molecule are displaced horizontally to give a rhomboidal cavity. In these cases, severe distortions of the host molecule were observed, and their energies were much higher than **2c**.

There are also many conformations having one or more torsion angles which depart substantially from ideal gauche and anti geometries. These permutations of the bridges lead to asymmetric structures (unlike **2a**−**c**). Each of these conformations somewhat modifies the shapes of the portals and the cavities; this can provide the host with a repertoire of cavities to accommodate various shapes of guest molecules. All of these conformers have energies higher than those of **2a**−**c**, which can be correlated with the orientation of the unshared electron pairs of the three adjacent oxygen atoms on the benzene rings of the polar caps.

As mentioned earlier, the orientation of the intrahemispheric bridges (OCH_2O) is important in determining how easy it is for molecules to pass in and out of the host.[23] The chair conformation has the central methylene group pointing toward the cavity (Figure 5a), while the boat form has the methylene group pointing away from the cavity (Figure 5b). In most conformers, for example, **2a** and **2c**, the chair form is more stable than the boat form by about 3.8 kcal/mol due to the repulsive 1,5-H interaction in the boat form. The energy barrier for the interconversion of one form to the other in **2a** or **2c** was estimated to be 12.0 kcal/mol by optimizing the structure with the phenyl carbon−oxygen−methylene carbon−oxygen torsional angle constrained to 0°.

In the case of **2b**, when the unshared electron pairs of three adjacent oxygen atoms of the benzene rings adopt an out−out−out orientation, the boat-conformation has a similar energy to the chair-conformation. This stabilization comes from the compensation of changing the orientation of the unshared electron pairs of the three adjacent oxygen atoms from an out−out−out orientation to an in−out−out orientation, which substantially reduces the dipole repulsion of these oxygen atoms. The barrier to conformational interconversion for **2b** is also calculated to be 12 kcal/mol.

In previous studies of a smaller carcerand using AMBER*, the chair-boat difference was calculated to be 7 kcal/mol, while the activation energy for chair-to-boat flip was predicted to be 22 kcal/mol.[23] Using the MM3* force field, these energies are predicted to be 4 and 12 kcal/mol, respectively. MM3* values for the conformational change are only about one-half those from AMBER*. These varying energies are representative of differences expected to be found using different force fields. The host previously studied has an O, CH_2, O pattern instead of having three adjacent oxygen atoms (Figure 2) on the aromatic ring, and electron-pair repulsion has a smaller differential effect on the energies of different conformations.

The relative energies of the different conformers of **2** may not be accurately predicted by MM3*, since no special parameterization of the MM3* force field has been performed for such molecules. It appears, however, that the guest molecules cause the host to assume the most accommodating shape, overcoming the relative small energy differences between conformers.

Thermodynamic Stabilities of Complexes. In previous studies of cavitands and hemispherands, Cram concluded that preorganization is one of the main factors determining the binding power of these host molecules.[6,7] Structural recognition also depends upon complementary stereoelectronic arrangement of host and guest molecules. Hemicarcerand **2** is highly preorganized with two rigid polar caps. However, the flexibilities of the four interhemispheric bridges give the host some latitude in the shape of portal and cavity, ranging from square to rhomboid to rectangular. This versatility allows the host

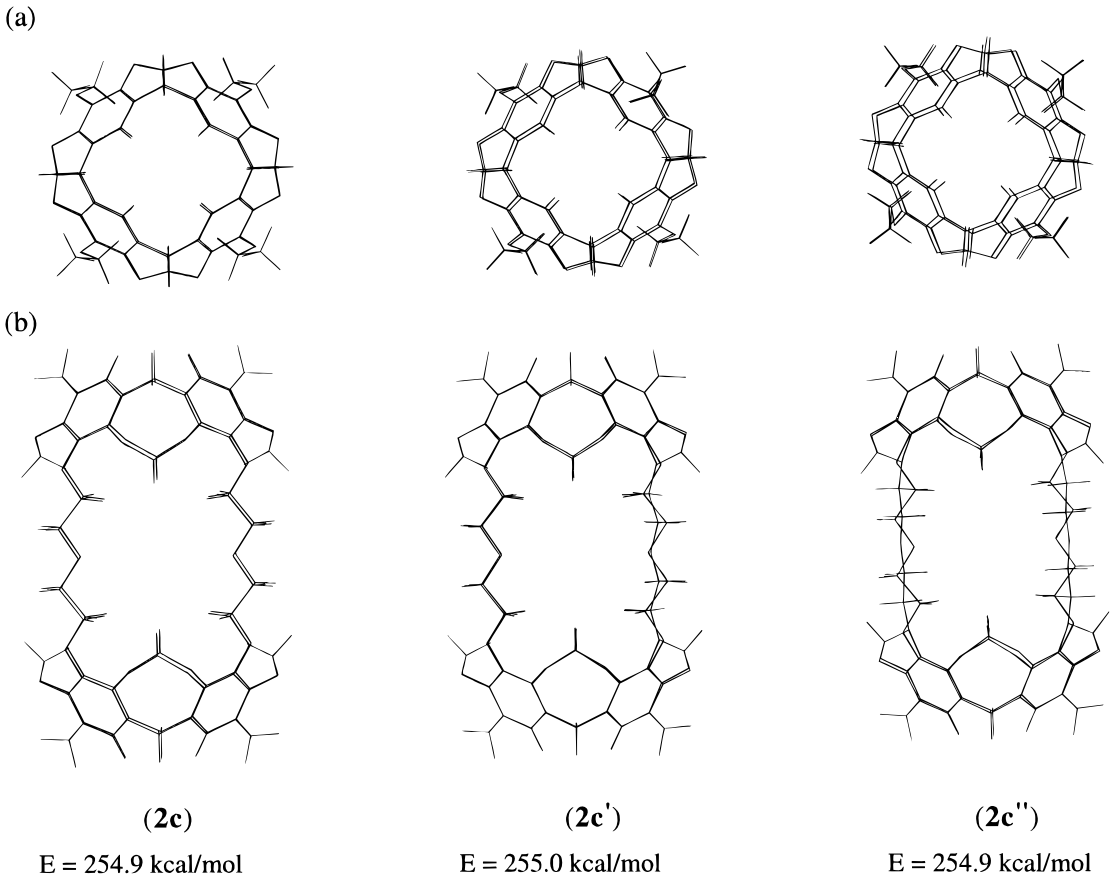

Figure 4. (a) Top view and (b) side view of **2** in different conformations.

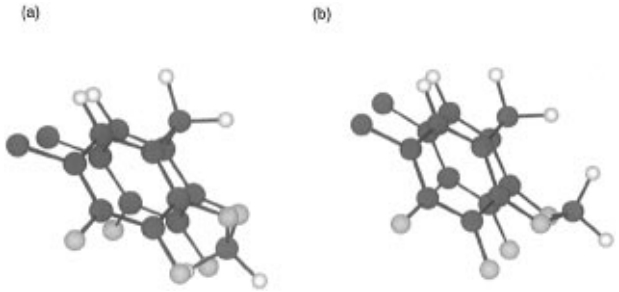

Figure 5. Orientations of methylene groups in the intrahemispheric bridges: (a) chair form and (b) boat form.

molecule the freedom to complement various shapes of guests. To quantitatively evaluate this complementarity, the energetics of the complexation process were carried out by molecular mechanics calculations and molecular dynamic simulations.

A. Molecular Mechanics Calculations. The complexes of 40 small organic molecules with hemicarcerand **2** were studied by molecular mechanics calculations with the MM3* force field. Starting geometries for the hemicarcerand-neutral guest complexes were obtained by docking the neutral guest inside the cavity of the hemicarcerand **2**. Although the host structures of **2a**−**c** are different in geometries and energies, very similar host

Table 1. MM3* Energies of Complexation of Hemicarcerand **2** with Various Neutral Bicyclic and Aromatic Guests

guest	E_{guest}	$E_{complex}$	ΔE_1[a]	guest[b] vol (Å^3)	guest	E_{guest}	$E_{complex}$	ΔE_1[a]	guest[b] vol (Å^3)
A1	37.4	267.1	−16.0	108.8	**B9**	8.2	233.9	−20.0	124.2
A2	32.1	263.4	−14.4	99.3	**B10**	8.9	233.6	−21.0	131.5
A3	72.8	306.0	−12.5	108.8	**B11**	7.0	230.6	−22.1	117.1
A4	39.0	266.9	−17.8	114.9	**B12**	8.2	231.7	−22.2	124.5
A5	39.7	268.5	−16.9	116.0	**B13**	9.7	234.1	−21.3	132.3
A6	38.7	268.6	−15.8	109.2	**B14**	5.8	236.2	−15.3	151.4
A7	38.1	268.9	−14.9	103.6	**B15**	11.8	243.6	−13.9	166.6
A8	47.9	279.2	−14.4	98.0	**B16**	5.8	229.8	−21.7	113.5
A9	25.6	251.3	−20.0	113.6	**B17**	6.3	229.4	−22.6	130.5
A10	12.7	236.9	−21.5	155.4	**B18**	5.9	231.1	−20.5	142.7
A11	20.0	242.8	−22.9	155.5	**B19**	7.5	231.6	−21.6	136.8
A12	11.7	238.9	−18.5	149.0	**B20**	6.7	234.8	−17.6	113.7
B1	6.2	236.9	−15.0	83.4	**B21**	14.7	247.8	−12.6	162.7
B2	5.5	231.6	−19.6	113.0	**B22**	38.5	266.2	−18.0	124.1
B3	5.9	236.2	−15.4	96.6	**B23**	39.3	266.4	−18.6	132.8
B4	7.5	234.0	−19.2	116.9	**B24**	42.4	269.4	−18.7	124.3
B5	8.9	233.3	−21.3	125.0	**B25**	46.3	269.6	−22.4	159.3
B6	7.3	235.9	−17.1	151.7	**B26**	27.8	256.6	−16.9	125.1
B7	14.7	239.5	−20.9	133.1	**B27**	20.5	249.2	−17.0	118.4
B8	17.7	247.6	−15.8	165.6	**B28**	39.0	268.1	−16.6	115.1

[a] $\Delta E_1 = E$(complex) − [E(host **2c**) + E(guest)]. [b] Guest volumes were calculated by using the "volume analysis" submode in the MACROMODEL program.

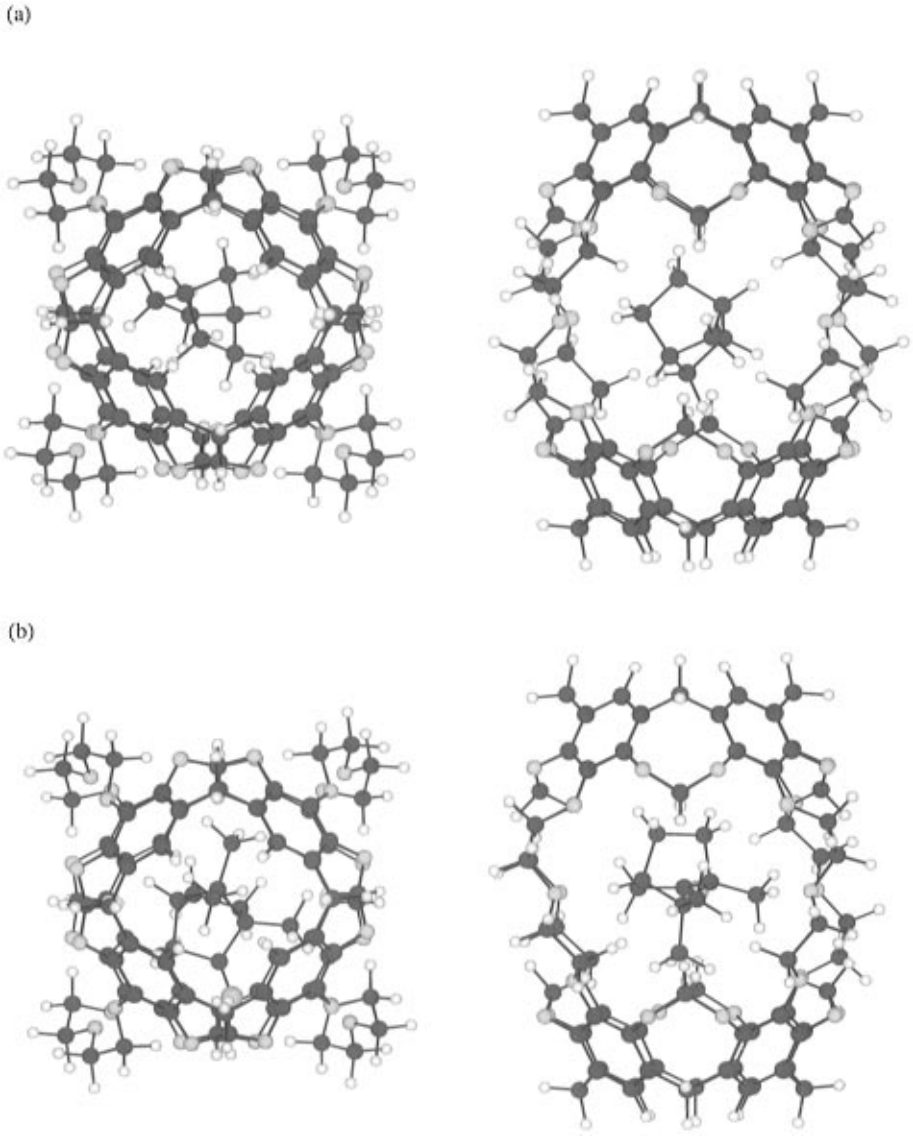

Figure 6. Top (right) and side (left) views of the molecular mechanics minimized structures of hemicarceplexes (a) **2⊙norbornane** (**2⊙A1**) and (b) **2⊙camphor** (**2⊙B25**).

geometries were obtained after minimizations of bicyclic guest complexes, regardless of the starting host geometry. The host has essentially the same geometry in the complexes as shown in **2c**. Note this is different from the host conformation in the hexa-aquo complex (Figure 3).

The energies of these complexes are dependent upon the orientations of the guest molecule inside the cavity. For the bicyclic guest molecules, molecular dynamics with the continuous simulated annealing method was employed to verify that the lowest energy conformer of each complex had been located. Complex stabilization energies were calculated from the difference between the energy of the best optimized complex and the sum of guest and host **2c**. The complexation energies are summarized in Table 1, along with the guest and complex energies, calculated by MM3*/MACROMODEL.[30] Guests marked a capital **A** are summarized in Chart 2 and form stable complexes with **2**, while those with a capital **B** are shown in Chart 3 and do not form isolable complexes with **2**. Table 1 also gives guest volumes, calculated with Still's algorithm.[30]

Our calculated results showed that the complexations of host **2** with bicyclic guests **A1**−**A9**, where stable complexes were observed experimentally, are energetically favorable by 12 to 20 kcal/mol (ΔE_1). Similar stabilization energies (ΔE_1 ranges from −17 to −22 kcal/mol) were also found for guests **B22** to **B28**, although none of these complexes were isolated experimentally.

These results suggest that the cavity inside the hemicarcerand is large enough to accommodate all the bicyclic guests studied here. Indeed, a closer look at the structures of these complexes show that the host moieties of these complexes have D_{2h} symmetry with four bridges expanding out in all cases. Examples of the MM3* optimized structures of hemicarceplexes **2⊙A1** (meaning guest **A1** in host **2**) and **2⊙B25** are shown in Figure 6.

As shown in Table 1, the uncomplexed bicyclic guests have larger volumes (115−159 Å^3) than the complexed ones (98−116 Å^3). However, the cavity of the host molecule can be expanded to accommodate the bicyclic guest as large as 159 Å^3 (Table 1, guest **B25**) without significant steric repulsions. The calculated complexation energies are similar for **A1**−**A9** and **B22**−**B28**. Since no X-ray structures of complexes of the above organic guests are currently available, the actual structures of the host−guest complex remain unknown, but the calculations provide predictions which we expect to be reasonable.[23]

Calculation of the complexes of **2** with aromatic guests, **A10**−**A11** and **B1**−**B21**, were also carried out. Although numerous

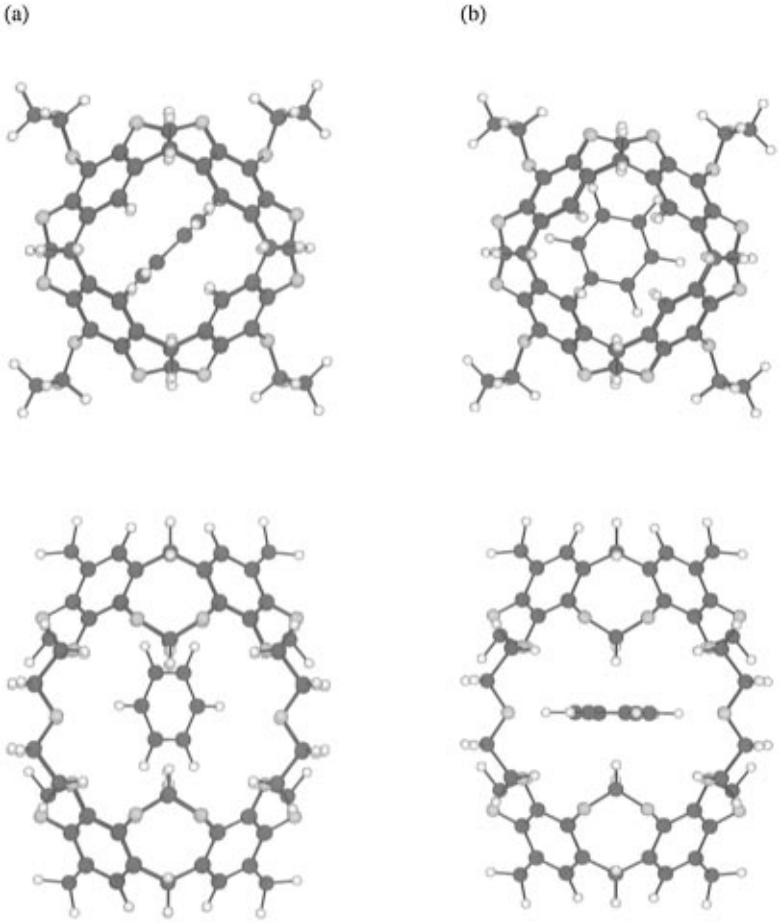

Figure 7. Top and side views of two distinct orientations of benzene guest with respect to host **2**.

Table 2. Components of Interaction Energies (kcal/mol) for Hemicarceplexes, **2⊙benzene** (**2⊙B1**) in Vertical and Horizontal Orientations

carceplexes	total E	$E_{stretch}$	E_{bend}	$E_{pro\ tor}$	$E_{electro}$	E_{VDW}
vertical	236.9	7.3	27.6	113.7	23.4	67.5
horizontal	239.0	7.4	26.7	113.6	24.3	69.6
ΔE^a	−2.1	−0.1	0.9	0.1	−0.9	−2.1

[a] $\Delta E = E_{vertical} - E_{horizontal}$. ΔE is further broken down into its bond stretching, angle bending, proper torsion, electrostatic, and van der Waals terms (Improper torsion term is relatively small and is not included here).

Table 3. Components of Interaction Energies (kcal/mol) for Hemicarceplexes, **2⊙*p*-diethoxybenzene** (**2⊙B15**) in Vertical and Horizontal Orientations

carceplexes	total E	$E_{stretch}$	E_{bend}	$E_{pro\ tor}$	$E_{electro}$	E_{VDW}
vertical	253.7	10.5	43.0	111.3	17.5	73.9
horizontal	243.6	8.7	36.1	107.5	17.4	76.4
ΔE^a	10.1	1.8	6.9	3.8	0.1	−2.5

[a] See Table 2.

orientations of the guests within the complex are possible, two distinct orientations of aromatic guests with respect to the host were found to be most important. These are shown in Figure 7. Figure 7a shows the optimized complex structure **2⊙B1**, where the axis of the host lies in the plane of guest. This is referred to as the "vertical orientation". Another conformer, referred to as the "horizontal orientation" (Figure 7b), has the plane of the guest perpendicular to the vertical axis of the host.

In most cases, the complex with vertical orientation is the lower energy conformer. For example, the horizontal orientation of **2⊙B1** is calculated to be 2.1 kcal/mol higher in energy than that of vertical orientation. The vertical orientation conformer of **2⊙B1** has larger electrostatic and van der Waals attractions between host and guest molecules (Table 2). The other energy components are nearly the same for the two guest conformations.

However, for the *p*-diethoxybenzene complex (**2⊙B15**), the vertical conformer is predicted to be 10.1 kcal/mol higher in energy than the horizontal. This high energy of the vertical orientation is due to the steric repulsion between the host and guest molecules at the polar region (Figure 8).

The energies of the two conformers are analyzed in Table 3. There are clear signs of nonbonded repulsions in the vertical conformer in the stretching and bending energy values.

The stabilization energies for hemicarcerand **2** with other aromatic guests were also calculated in a similar fashion. The results are summarized in Table 1. Complexation energies of the complexed (**A10** and **A11**) and the uncomplexed aromatic guests (**B1**−**B21**) with host **2** are calculated all to be energetically favorable by 13−23 kcal/mol (ΔE_1). The volumes of these guests range from 83.4 Å^3 for benzene (**B1**) to 166.6 Å^3 for diethoxybenzene (**B15**). The two complexed aromatic guests (**A10** and **A11**) have very similar volumes (155.5 Å^3) and stabilization energies (−21.5 and −22.9 kcal/mol). There is no correlation between guest volume and the observation of a complex.

To summarize this section, all of the guest molecules shown in Charts 2 and 3 are predicted to form stable complexes with **2**, with binding energies of 12−23 kcal/mol. There must be reasons other than thermodynamics which cause the guests in Chart 2 to give isolable complexes, while those in Chart 3 do not.

B. Molecular Dynamic Simulations. In the molecular mechanics calculations, only the energies of the lowest energy

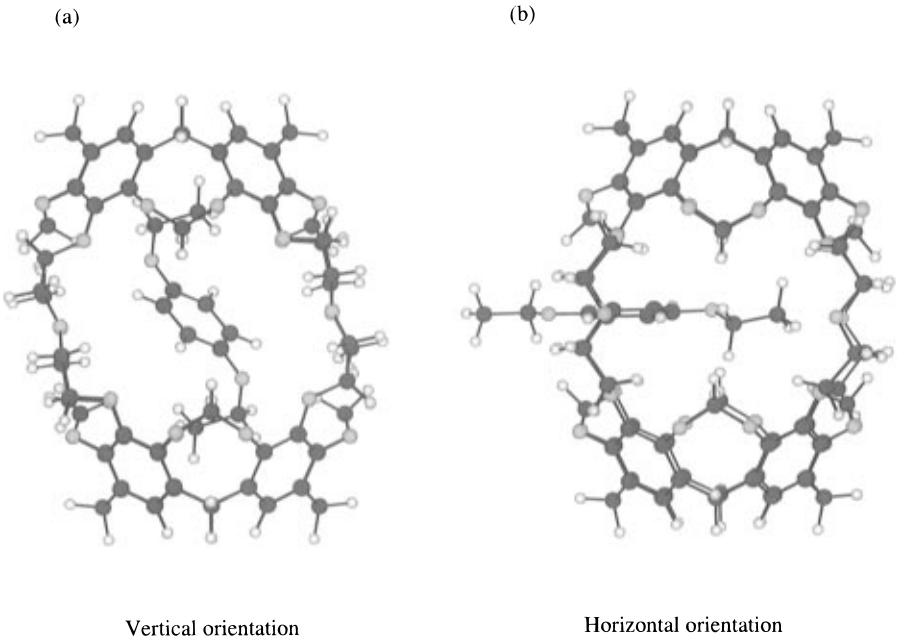

Figure 8. Two distinct orientations of *p*-diethoxybenzene guest with respect to host **2**.

Table 4. Average Enthalpies for Host-Guest Complexation[a]

guest	energy of guest (kcal/mol)	energy of host (kcal/mol)	energy of complex (kcal/mol)	ΔE (kcal/mol)
norbornane	77.6 ± 0.5	645.6 ± 2.1	711.3 ± 2.3	−11.9 ± 2.3
camphor	104.5 ± 0.7	645.6 ± 2.1	734.4 ± 2.3	−15.7 ± 2.3

[a] ΔE = *E*(complex) − [*E*(host) + *E*(guest)].

structure for each complex was compared. In order to scan a larger part of the conformational space of the hemicarceplex, a molecular dynamics evaluation of the average enthalpy was performed using the MACROMODEL program. Two complexes were studied, involving complexation between host **2** and guests **A1** and **B25**. **A1** is relatively small and forms a stable complex, while **B25** is the largest bicyclic guest studied and does not form a complex. The simulations were run at 373 K with timestep of 0.5 fs and equilibrium time of 5 ps before each dynamics run. The total simulation times are 20, 100, and 200 ps for guest, host, and complex, respectively. The results are summarized in Table 4.

The average enthalpies of complexation for guests **A1** and **B25** are −11.9 ± 2.3 and −15.7 ± 2.3 kcal/mol, respectively. These values can be compared to ΔE_1 values of −15.2 and −19.5 kcal/mol for **A1** and **B25** in Table 1. Both molecular mechanics and molecular dynamics results indicate that both the complexation processes are energetically favorable, although the average enthalpies of complexation are less negative. This is a reflection of the fact that the host−guest complex is an average of the global minimum and a number of higher energy conformers. Most significantly, there is no correlation between complex stability and the observation of a complex.

Estimation of Solvation Effects. The complexation energies in Table 1 are for the gas-phase and do not include solvation energies. The solvation energies of the empty hosts are most likely similar to those of the hosts bearing guests, and these have not been calculated. Upon complexation, a guest is removed from solvent and inserted into the host. This loss of guest solvation energy is a significant contribution to the energetics of complexation. The total change in solvation energy upon complexation is approximated here from the guest solvation energy alone. The solvation energies of liquid guest molecules are approximately equal to their vaporization energies and can be estimated by Trouton's rule.[33] For sublimable guests, the solvation energies were estimated as the sublimation energies, calculated as $\Delta E_2 = 2.303\mathrm{R} \times \mathrm{B}$, where the parameter *B* is from the best data in the literature, expressed in the form $\log_{10} P = A - B/T$.[34]

Table 5. Estimated Solvation Energies (kcal/mol) and MM3* Energies (kcal/mol) of Complexation of Hemicarcerand **2** with Various Neutral Bicyclic and Aromatic Guests

guest	ΔE_1[a]	ΔE_2[b]	ΔE_3[f]	guest	ΔE_1[a]	ΔE_2[b]	ΔE_3[f]
A1	−16.0	7.9[d]	−8.1	**B9**	−20.0	9.4[d]	−10.6
A2	−14.4	8.3[d]	−6.1	**B10**	−21.0	10.2[d]	−10.8
A3	−12.5			**B11**	−22.1	8.5[c]	−13.6
A4	−17.8	9.5[d]	−8.3	**B12**	−22.2	9.4[d]	−12.8
A5	−16.9			**B13**	−21.3	10.1[d]	−11.2
A6	−15.8	9.3[d]	−6.5	**B14**	−15.3	9.6[d]	−5.7
A7	−14.9	7.8[d]	−7.1	**B15**	−13.9	10.7[d]	−3.2
A8	−14.4	7.6[d]	−6.8	**B16**	−21.7	9.4[d]	−12.3
A9	−20.0			**B17**	−22.6	10.3[d]	−12.3
A10	−21.5	11.1[d]	−10.4	**B18**	−20.5	11.7[d]	−8.8
A11	−22.9	10.8[d]	−12.1	**B19**	−21.6	10.8[d]	−10.8
A12	−18.5			**B20**	−17.6	10.8[d]	−6.8
B1	−15.0	7.3[c]	−7.7	**B21**	−12.6	11.2	−1.4
B2	−19.6	9.7[d]	−9.9	**B22**	−18.0		
B3	−15.4	10.9[d]	−4.5	**B23**	−18.6	9.6	−9.0
B4	−19.2	8.7[c]	−10.5	**B24**	−18.7	10.7	−8.0
B5	−21.3	9.4[d]	−11.9	**B25**	−22.4	12.8[e]	−9.6
B6	−17.1	9.6[d]	−7.5	**B26**	−16.9		
B7	−20.9	10.2[d]	−10.7	**B27**	−17.0		
B8	−15.8	10.7[d]	−5.1	**B28**	−16.6		

[a] ΔE_1 = *E*(complex) − [*E*(host **2c**) + *E*(guest)]. Data repeated from Table 1 for comparison. [b] ΔE_2 = vaporization energies for guest molecules. [c] Experimental values. [d] Estimated by Trouton's rule.[27] [e] For sublimable guests, the ΔE_2 were calculated as their sublimation energies. [f] $\Delta E_3 = \Delta E_1 + \Delta E_2$.

The estimated solvation energies for guests in the liquid are listed in Table 5. For bicyclic guests, the values range from 7.6 to 12.8 kcal/mol. The large bicyclic molecules, **B23**−**B25**, do have larger solvation energies (range from 9.6 to 12.8 kcal/mol) than the smaller molecules (from 7.6 to 9.5 kcal/mol), but the differences are not large enough to account for the fact that **A1**−**A9** form complexes and **B22**−**B28** do not. The solvation energies for aromatic guests are also very similar, ranging from 7.3 to 11.7 kcal/mol. Again, the differences in solvation energies for complexed and uncomplexed guests are not large enough to explain the differences.

The molecular mechanics and molecular dynamics calculations show that the complexation of hemicarcerand **2** with two

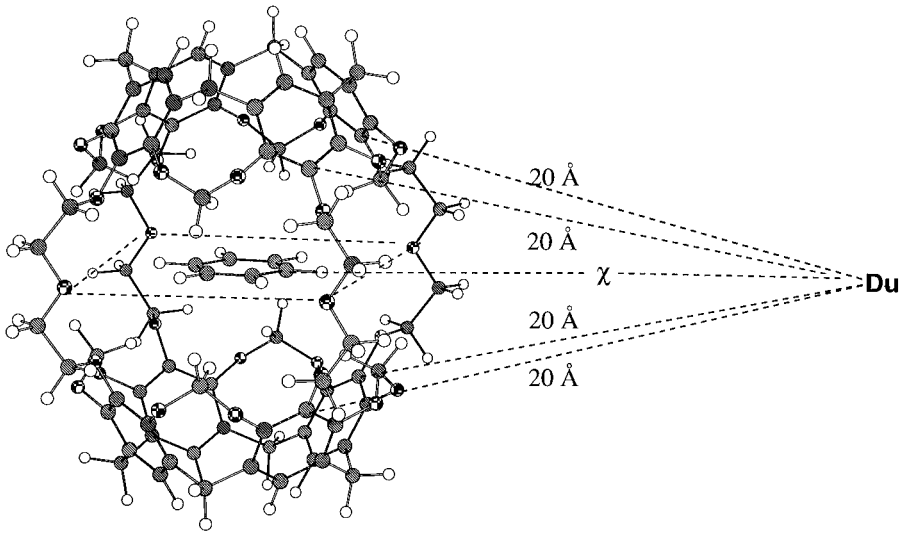

Figure 9. Definition of reaction coordinate, χ, for the reaction path calculations.

classes of guests studied here are all energetically favorable. Even taking into account the solvation energies of guest molecules, the complexation of all guests are still energetically favorable. The entropies of complexation also need to be considered in order to know whether the free energy of complexation is negative. Although the free energies of complexation of a guest by an empty host in the gas phase would be negative by 30−50 eu, the complexation in solution is expected to have entropies of complexation much closer to zero. Experimental entropies of complexation have not been measured for the molecules studied here, but for the related hemicarceplexes the values range from −13.6 to −19.4 eu.[20] This is because the desolvation of the guest has a favorable entropy. It is also likely that an empty host molecule never actually exists, except under anhydrous conditions in a bulky solvent. The gas phase energy of complexation of chloroform was calculated, since this solvent has been used in the purification procedure. The complexation energy of one $CHCl_3$ in the gas phase is 13.9 kcal/mol, while for two $CHCl_3$ molecules the energy is 22.4 kcal/mol. The solvation energy of $CHCl_3$ is 7.5 kcal/mol, and so chloroform will form slightly stable complexes.

Since estimated thermodynamics stabilities do not correlate with observed stabilities in any obvious way, the kinetics of complex formation were investigated.

Kinetics of Complexation and Decomplexation. Calculations were performed to estimate the activation energies for guest escape processes. A reaction coordinate, χ, was defined to force the guest through the equatorial portal. Previous work showed that the axial portals are too small to allow egress of organic guests.[23] As illustrated by the dotted lines in Figure 9, a dummy atom was placed at 20 Å away from the four phenyl carbons of the host molecule, and the distance between one atom of the guest molecule and the dummy atom was taken as the reaction coordinate. By gradually decreasing the distance between the guest molecule and the defined dummy atom, the activation energy for the guest escape process was estimated by energy minimizations for each step.

Figures 10 and 11 are two examples of the energy versus reaction coordinate diagrams, calculated in this way, for the complexation/decomplexation of norbornane (**A1**) and camphor (**B25**) guests with host **2**. For the host molecule with all intrahemispheric bridges in the favored chair conformation, the calculated decomplexation energy barriers are 41 and 57 kcal/mol for guests **A1** and **B25**, respectively. The complexation activation energies (neglecting solvation) are 28 and 41 kcal/mol, respectively. These activation energy barriers are much too high for either complexation or decomplexation to occur near room temperature.

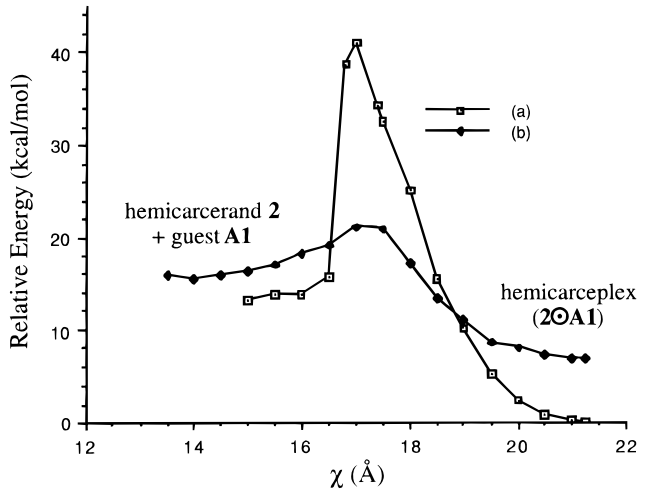

Figure 10. Energy profile for the decomplexation of norbornane (**A1**): (a) All intrahemispheric bridges in chair conformations and (b) two intrahemispheric bridges in boat conformation.

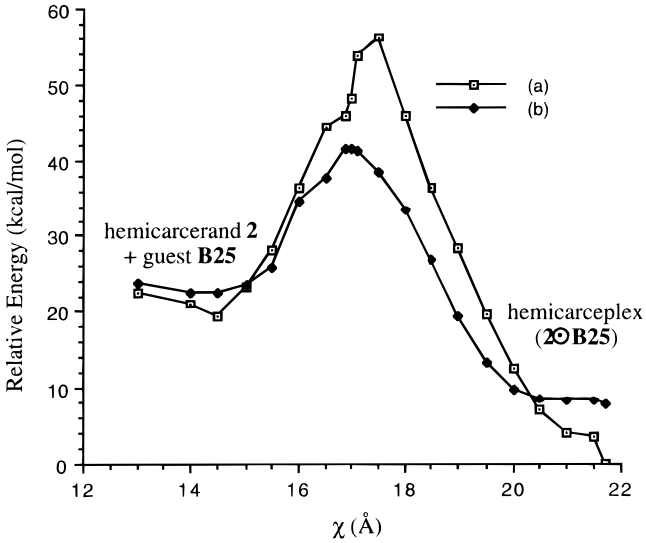

Figure 11. Energy profile for the decomplexation of camphor (**B25**): (a) All intrahemispheric bridges in chair conformations and (b) two intrahemispheric bridges in boat conformation.

As shown in earlier work with a related hemicarceplex, the conformations of the intrahemispheric OCH_2O linkages can

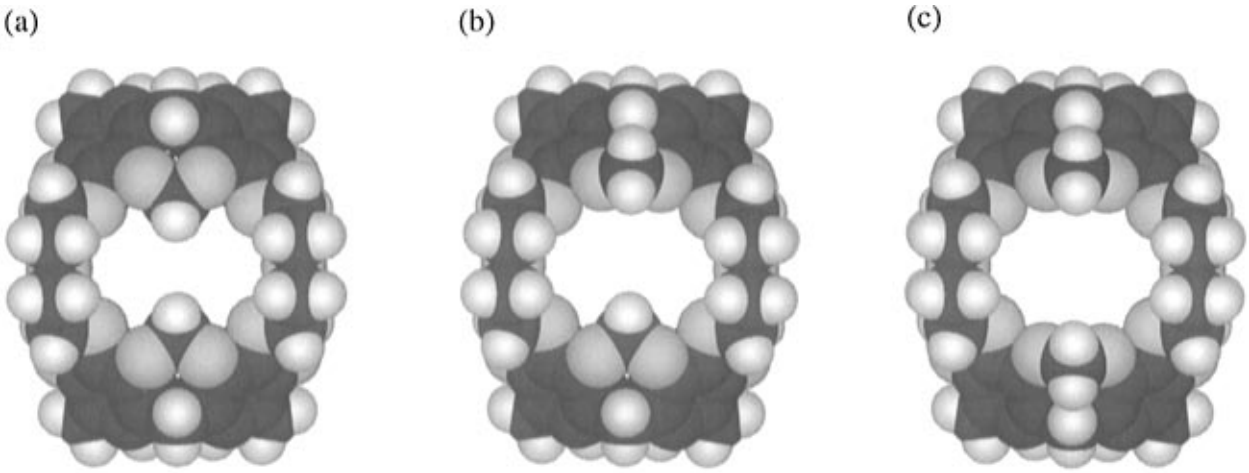

Figure 12. CPK models for hemicarcerand **2** with (a) two chair forms, (b) one chair and one boat form, and (c) two boat forms.

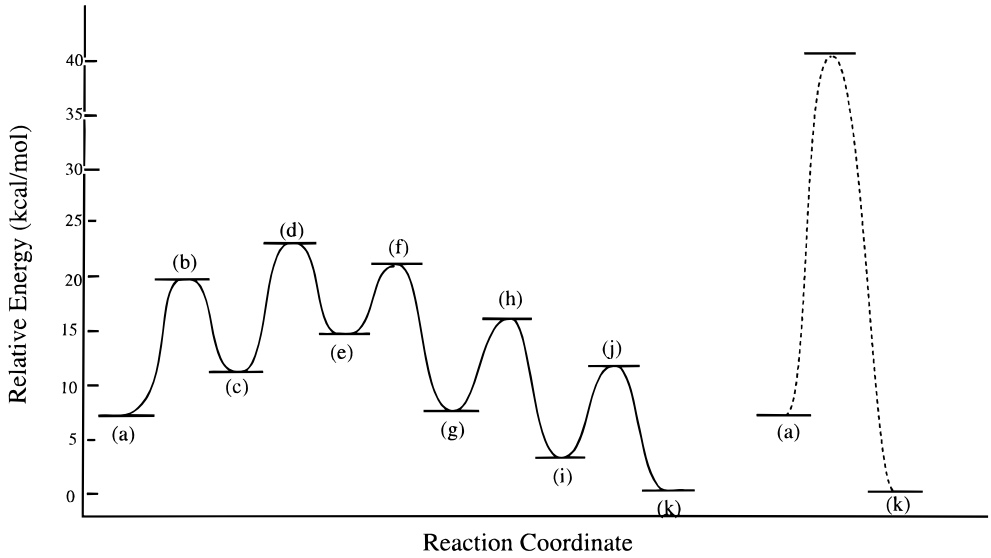

Figure 13. Energy profiles for the complexation of hemicarceplex **2** with norbornane (**A1**) by the stepwise mechanism (left, full line) and the one-step mechanism (right, dashed line): (a) hemicarcerand **2**; (b) transition state for one chair-boat flip; (c) hemicarcerand **2** with one boat form; (d) transition state for second chair-boat flip; (e) hemicarcerand **2** with two boats; (f) transition state for the complexation of guest **A1**; (g) **2**⊙**A1** with two boat forms; (h) **2**⊙**A1** with one intrahemispheric bridge adopting the boat form and the second at the transition state for boat-chair flip; (i) **2**⊙**A1** with one boat form; (j) **2**⊙**A1** with one bridge adopting the chair form and the other in transition state for boat-chair flip; and (k) **2**⊙**A1**. Note that above energies are MM3* except an estimated solvation energy of −7.9 kcal/mol had been added to points (a)−(e).

greatly influence the activation energy.[23] A chair to the boat conformational flip (Figure 5) increases the size of the equatorial portal, permitting more facile passage of guest molecules in and out of the cavity. Figure 12 shows space-filling computer models of hemicarcerand **2** with the two visible intrahemispheric linkages in chair and boat conformations.

Starting from the lowest energy conformer of the hemicarcerand, **2c**, the complexation and decomplexation activation energies calculated for norbornane are 28 and 41 kcal/mol, respectively (Figure 10). When the portal is enlarged by flipping two intrahemispheric OCH_2O linkages from the chair conformer to boat form, the barriers become very low, 6 and 21 kcal/mol, respectively.

According to MM3*, the chair conformer is 3.8 kcal/mol more stable than the boat. The activation barrier to conformational interconversion is estimated to be 12 kcal/mol. The opening of the second flap of the portal requires an additional activation energy of 12 kcal/mol, and a fully-opened portal is 7.6 kcal/mol above the closed portal.

Figure 13 shows the full energy profiles for both stepwise and one-step complexation/ decomplexation processes. These calculations come from MM3* optimization with a correction for guest solvation energy of hemicarcerand **2** with guest **A1**. That is, an estimated 7.9 kcal/mol of guest (**A1**) solvation energy has been added to the MM3* energies. The first set of energy contours represent passage from **2** to **2**⊙**A1** by first opening an equatorial portal from chair to boat conformation of the intrahemispherical methylene linkage (see caption in Figure 13). It is clear that the activation energy in complexation of guest **A1** (a → f) is only 16 kcal/mol for the stepwise mechanism, while the E_a for a one-step mechanism is 34 kcal/mol. The energy of the transition state for the second chair-boat flip (d, Figure 13) is slightly higher than that of transition state of guest complexation (f, Figure 13). Thus, the rate-determining step in complexation of guest **A1** is predicted to be the gate-opening.

The energy profiles for both stepwise and one-step complexation processes of hemicarcerand **2** with guest **B25** are also shown in Figure 14. The stepwise process is also calculated to be lower in activation energy than the one-step process without portal opening. The activation energy for the complexation of bigger guest **B25** via the stepwise mechanism is still calculated to be very high, 35 kcal/mol, which is about 19 kcal/mol higher than that of complexation of guest **A1**. The results suggest that the activation energy for the complexation of guest **B25** with **2** is too high to form a complex under the experimental conditions which have been tried so far.

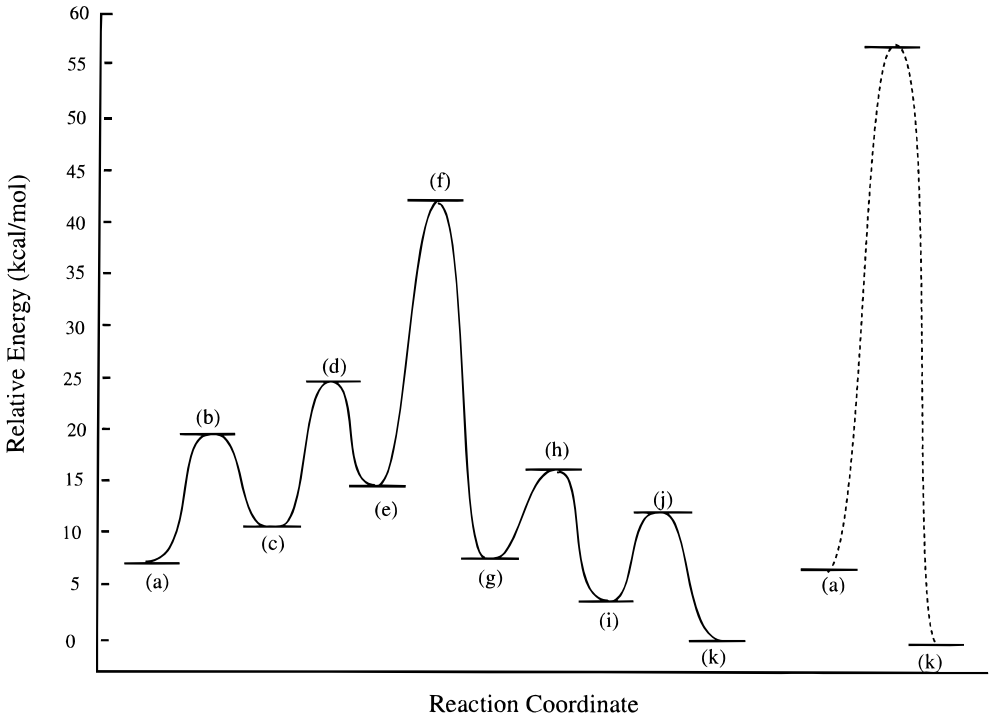

Figure 14. Energy profiles for the complexation of hemicarceplex **2** with guest camphor (**B25**) by the stepwise mechanism (left, plain line) and the one-step mechanism (right, dashed line). Each letter has the same meaning as Figure 13. Note that above energies are MM3* except an estimated solvation energy of −12.8 kcal/mol had been added to points (a)−(e).

Table 6. Results of Molecular Mechanics Calculations on the Complexation of Hemicarcerand (**2**) with Xylenes and Their Decomplexation Energies

guest	E_{guest} (kcal/mol)	E_{host} (kcal/mol)	$E_{complex}$ (kcal/mol) vertical	$E_{complex}$ (kcal/mol) horizontal	E_{vap}[a] (kcal/mol)	ΔE_1[b] (kcal/mol)	ΔE_2[c] (kcal/mol)	E_d[d] (kcal/mol)
p-xylene	7.0	245.7	230.6	238.9	8.5	−13.6	−8.3	15.7
m-xylene	7.0	245.7	234.7	236.8	8.5	−9.5	−2.1	13.1
o-xylene	7.5	245.7	234.0	235.8	8.7	−10.5	−1.8	13.7

[a] E_{vap} = enthalpies of vaporization of compounds at their normal boiling point (defined at a pressure of 101.325 kPa). Data were taken from reference. [b] $\Delta E_1 = E_{complex}(\text{vertical}) - [E_{guest} + E_{host(2)} - E_{vap}]$. [c] $\Delta E_2 = E_{complex}(\text{vertical}) - E_{complex}(\text{horizontal})]$. [d] E_d = activation energies for the decomplexation of xylene guests from host (**2**); calculated by reaction coordinate method.

Figure 15 shows the structures and the space-filling models of **2**⊙**A1** and **2**⊙**B25** at its transition state. It is clear that even with the two intrahemispherical methylene bridges open, the guest **B25** is still in close contact with the host molecule at the portal region.

These results give a plausible explanation for why small bicyclics **A1**−**A9** can form complexes. The energetics in these cases appear to all be very similar. The large bicyclics **B22**−**B28** are sufficiently large so that the activation energy for complex formation will be quite high. This does not explain the difference between the aromatics **A10** and **A11**, which do form complexes, and **B1**−**B21**, which do not.

To explore these cases, the activation energies for the complexation of benzene and toluene guests were also carried out by the reaction coordinate method.

Molecular mechanics calculations show that the complexation energies (ΔE_1) for hemicarcerand **2** with benzene and toluene guests are −15.2 and −16.7 kcal/mol, calculated as $\Delta E_1 = E(\text{complex}) - [E(\text{host } \mathbf{2c}) + E(\text{guest})]$, respectively. The molar vaporization energies, estimated by Trouton's rule, for benzene and toluene are 7.5 and 8.1 kcal/mol, respectively. By including these solvent stabilizations, the corrected complexation energies for benzene and toluene from the liquids are −7.7 and −8.6 kcal/mol, respectively.

Since benzene and toluene guests are disk-shaped, the horizontal orientation shown in Figure 7 would provide the least steric hindrance during complexation and decomplexation processes. The energy profiles for the decomplexation of guests from both vertical and horizontal orientations were performed and compared. In both cases, rotations from the vertical orientation to the horizontal orientation were observed during the constrained optimizations.

The energy barriers for the decomplexation of benzene guest were calculated to be 11.0, 11.1, and 12.7 kcal/mol, when the intrahemispheric bridges are all chair forms, when one is a boat form and when two are boat forms, respectively (Figure 16). These values are all very small, and the opening of the portal has essentially no effect on the barriers. There is no barrier to complexation. The barrier for decomplexation is essentially the same as the complexation energy, and so there is no constrictive binding. Very similar results were obtained for toluene as guest. These data are not shown since they are nearly identical.

A similar analysis was carried out for disubstituted benzene derivatives. The thermodynamic stability and activation energy for the decomplexation of xylene guests with hosts **2** were evaluated; the results are summarized in Table 6.

Complexation between host **2** and the xylenes are energetically favorable by 9.5−13.6 kcal/mol (Table 6, ΔE_1). The complexes of **2** with xylene guests are expected to be thermodynamically stable. However, the relatively low decomplexation barriers (Figure 17) may cause the loss of guest molecules during the chromatographic purification.

The complexation of dimethoxybenzene guests with hemicarcerand **2** were also analyzed in a similar manner. Results

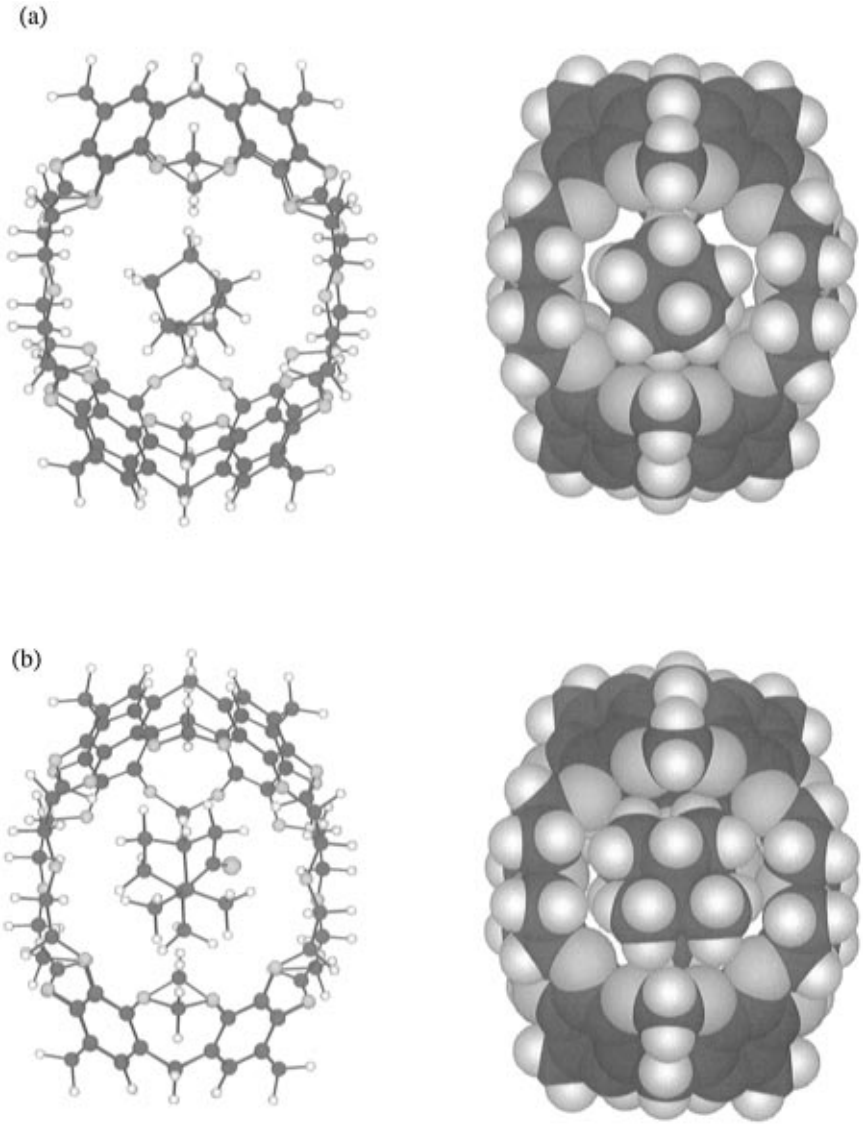

Figure 15. Transition-state structures for formation of (a) **2⊙norbornane** and (b) **2⊙camphor** from host and guest. The space-filling models are shown on the right.

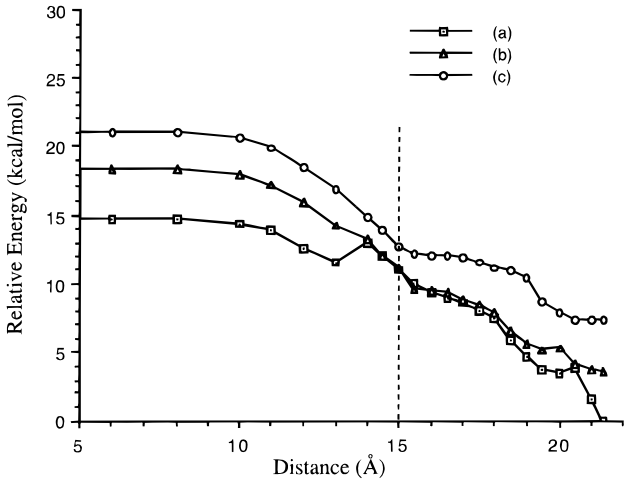

Figure 16. Energy profile for the complexation and decomplexation of benzene guest in vacuo: (a) both intrahemispheric bridges in chair form, (b) one intrahemispheric bridge in chair form and one in boat form, and (c) both intrahemispheric bridges in boat form. Guest is completely out of the host cavity at a distance shorter than 15.0 Å.

of the thermodynamic stabilities and the kinetics of the complexation of dimethoxybenzene guests with host **2** are summarized in Table 7 and Figure 18.

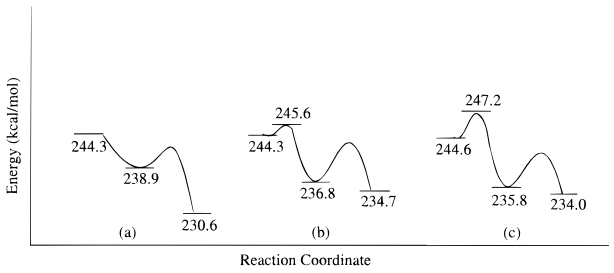

Figure 17. Energy profiles for the complexation of hemicarcerand (**2**) with (a) *p*-xylene, (b) *m*-xylene, and (c) *o*-xylene as guest. In each case, the complexation process starts from left to right. Two minima correspond to the complex having the guest in horizontal- (middle) and vertical-orientation (right), respectively. Note above energies are MM3* except solvation energies of −8.8, −8.5, and −8.7 kcal/mol had been added to the starting point of spectra (a), (b), and (c), respectively.

Complexations between host **2** and dimethoxybenzenes are also found to be energetically favorable by 9.6−11.2 kcal/mol (Table 7, ΔE_1). The decomplexation barriers for the dimethoxybenzene guests from host **2** were examined, and all three guests were found to have similarly low values (Table 6, E_d), with a slightly higher energy barrier for *o*-dimethoxybenzene. Thus, the fact that these complexes are not isolable experimentally comes as no surprise since the decomplexation process is

Table 7. Results of Molecular Mechanics Calculations on the Complexation of Hemicarcerand (**2**) with Dimethoxybenzene and Their Decomplexation Energies

guest	E_{guest} (kcal/mol)	E_{host} (kcal/mol)	$E_{complex}$ (kcal/mol) vertical	$E_{complex}$ (kcal/mol) horizontal	E_{vap}[a] (kcal/mol)	ΔE_1[b] (kcal/mol)	ΔE_2[c] (kcal/mol)	E_d[d] (kcal/mol)
p-dimethoxybenzene	9.7	245.7	234.1	240.3	10.1	−11.2	−6.2	11.3
m-dimethoxybenzene	8.9	245.7	233.6	239.0	10.2	−10.8	−5.4	13.4
o-dimethoxybenzene	13.6	245.7	239.5	240.4	10.2	−9.6	−0.9	16.0

[a] E_{vap} = enthalpies of vaporization of compounds at their normal boiling point estimated by Trount's rule. [b] $\Delta E_1 = E_{complex}(\text{vertical}) - [E_{guest} + E_{host(2)} - E_{vap}]$. [c] $\Delta E_2 = E_{complex}(\text{vertical}) - E_{complex}(\text{horizontal})]$. [d] E_d = activation energies for the decomplexation of dimethoxybenzene guests from host (**2**); calculated by reaction coordinate method.

Table 8. Results of Molecular Mechanics Calculations on the Complexation of Hemicarcerand **2** with 1-Bromo-3,4-dimethoxybenzene (**A10**) and 1,2,3-Trimethoxybenzene (**A11**) and Their Decomplexation Energies

guest	E_{guest} (kcal/mol)	E_{host} (kcal/mol)	$E_{complex}$ (kcal/mol) vertical	$E_{complex}$ (kcal/mol) horizontal	E_{vap}[a] (kcal/mol)	ΔE_1[b] (kcal/mol)	ΔE_2[c] (kcal/mol)	E_d[d] (kcal/mol)
A10	12.7	245.7	236.9	241.4	11.1	−10.4	−4.5	18.8
A11	20.0	245.7	242.8	250.1	10.8	−12.1	−7.3	26.7

[a] E_{vap} = enthalpies of vaporization of compounds at their normal boiling point estimated by Trount's rule. [b] $\Delta E_1 = E_{complex}(\text{vertical}) - [E_{guest} + E_{host(2)} - E_{vap}]$. [c] $\Delta E_2 = E_{complex}(\text{vertical}) - E_{complex}(\text{horizontal})]$. [d] E_d = activation energies for the decomplexation of 1-bromo-3,4-dimethoxybenzene and 1,2,3-trimethoxybenzene guests from host (**2**); calculated by reaction coordinate method.

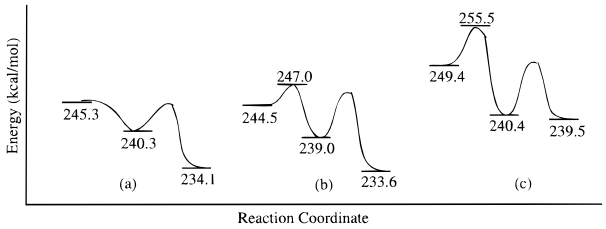

Figure 18. Energy profile for the complexation of dimethoxybenzene and hemicarcerand (**2**): (a) *p*-dimethoxybenzene, (b) *m*-dimethoxybenzene, (c) *o*-dimethoxybenzene as guest. In each case, the complexation process starts from left to right. Two minima correspond to the complex having the guest in horizontal- (middle) and vertical-orientation (right), respectively. Note above energies are MM3* except solvation energies of −10.1, −10.2, and −10.2 kcal/mol had been added to the starting point of spectra (a), (b), and (c), respectively.

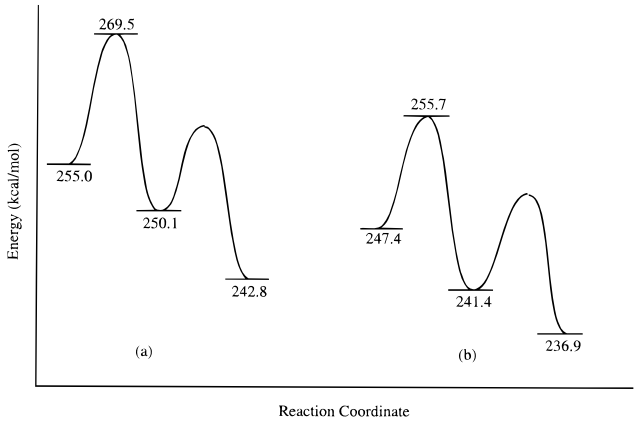

Figure 19. Energy profile for the complexation of hemicarcerand **2** with (a) 1,2,3-trimethoxybenzene and (b) 1-bromo-3,4-dimethoxybenzene as guest. In each case, the complexation process starts from left to right. Two minima correspond to the complex having the guest in horizontal- (middle) and vertical-orientation (right), respectively. Note above energies are MM3* except solvation energies of −10.8 and −11.1 kcal/mol had been added to the starting point of spectra (a) and (b), respectively.

very easy, similar to the cases of benzene or xylene as guests. The experimental observation[24] of an unstable *o*-dimethoxybenzene−host complex during the isolation and purification may be attributed to its slightly higher decomplexation energy barrier.

Experimentally, 1-bromo-3,4-dimethoxybenzene (**A10**), and 1,2,3-trimethoxybenzene (**A11**) are the two trisubstituted aromatic guests that can form stable complexes with **1**. Thermodynamic stabilities and kinetic decomplexation of these complexes were also examined as before and the results are summarized in Table 8.

The complexation energies of **2**⊙**A10** and **2**⊙**A11** are −10.4 and −12.1 kcal/mol, respectively. The decomplexation activation energies (E_d) for both guests were calculated to be moderate and are 26.7 and 18.8 kcal/mol (Figure 19), respectively. These results support the idea that constrictive binding energy is necessary to obtain stable complexes.

Although our calculations did not include entropy effects, and our estimation of the solvation energies may be crude, we believe that these effects should be similar for similar guests. Thus, in contrast to the uncomplexed bicyclic guests (**B22**−**B28**), which do not form complexes due to the high activation barriers for complexation, small aromatic guests readily form complexes in solution, but rapidly undergo decomplexation upon attempted purification. Only the aromatic molecules with several substituents are bulky enough to require gate opening. Smaller aromatics pass in and out without additional barriers. There is no constrictive binding of small aromatics. Thus the gating effect of the 1,3-dioxocyclocta-4,7-diene rings is critical in combining constrictive binding with host cavity accessibility. In the absence of the gate, guests can be trapped only upon synthesis: true carceplexes which do not lose guests are the result. Large portals (perpetually open gates) do not afford constrictive binding. Gates which open and close with moderate activation energies afford hemicarceplexes which form stable complexes with moderately-sized organic guests.

To prevent the competition between complexation by guest and solvent, complex formation can be carried out by heating the host molecules with neat liquid guests at refluxing temperatures. Alternatively, complexation of solid guests can also be achieved by dissolving the guests in a bulky solvent. Diphenyl ether has been used extensively for this purpose, since this molecule has a butterfly-shape geometry and is thought to be too large to enter the host interior. This solvent has also been used in the complexation studies of hemicarcerand **1**.[24] Our modeling studies show that diphenyl ether can easily fit into the host's cavity to form a complex with host **2** (Figure 20), with a stabilization energy of 12.6 kcal/mol. Taking into account the solvation energy of 11.2 kcal/mol for diphenyl ether, this value becomes only 1.4 kcal/mol, the smallest of the values in Table 5.

The activation energies for the decomplexation of diphenyl ether guest, calculated by the constrained optimization method,

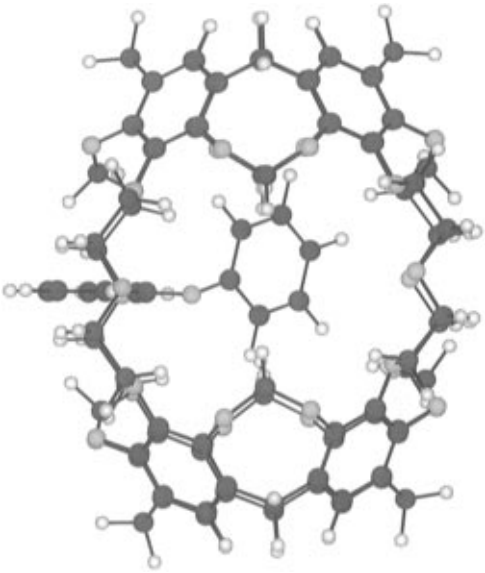

Figure 20. Hemicarceplex of host **2** with diphenyl ether as guest.

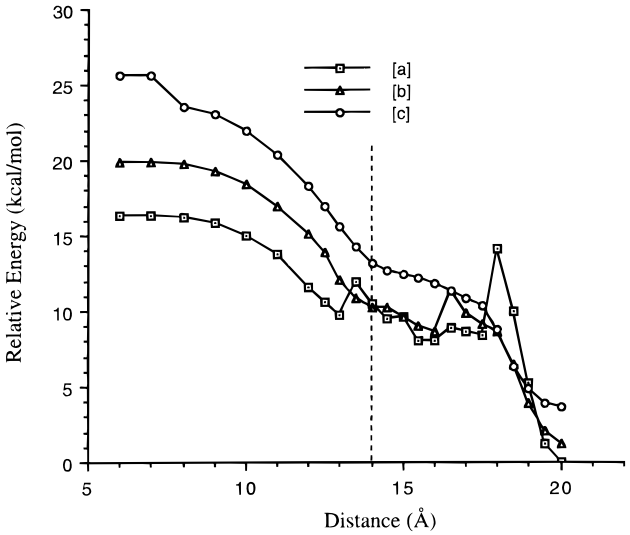

Figure 21. Energy profile for the decomplexation of diphenyl ether guest in vacuo: (a) both intrahemispheric bridges in chair form, (b) one intrahemispheric bridge in chair form and one in boat form, and (c) both intrahemispheric bridges in boat form. Guest is completely out of the host cavity at the distance shorter than 14 Å.

are 14.4, 11.4, and 12.7 kcal/mol (Figure 21) for the host molecule with the intrahemispheric bridges both at chair forms, one chair form, and both at boat forms, respectively. Corrected for solvation, there are no constrictive barriers to decomplexation. These values are relatively small and are similar to the calculated decomplexation energies for the benzene guest (Figure 16). Large excesses of diphenyl ether solvent would interfere slightly with the complexation of small aromatic guests, when the complexes are only a few kcal/mol more stable than the uncomplexed guest and host.

Summary

The structures and stabilities of 1:1 complexes of hemicarcerand **2** with two classes of guests have been examined. Three distinct structural geometries of hemicarcerand **2** are located during structural optimizations. The energies and geometries of the host molecule optimized by molecular mechanics are found to be highly dependent on the orientations of the three oxygen atoms attached to the benzene rings. The flexibilities of the interhemispheric linkages ($OCH_2CH_2OCH_2CH_2O$) provide hemicarcerands **1** and **2** with versatile binding abilities to accommodate various shapes of guests, ranging from spherical to rhomboidal to disk-shaped.

The interconversion of the intrahemispheric bridges (OCH_2O) of the host molecule from the chair form to the boat form serves as the transient opening of a gate for passage of guest molecules in and out of the hemicarceplex. This stepwise mechanism was found to be lower in energy than the one-step process, unless the guest is very small. The gate affords constrictive binding when closed and ready access to the cavity when open.

The thermodynamic stability for the complexations of **2** with both classes of guests are found to be very similar. Bicyclic guests **A1**−**A9** form stable complexes with **2** because they can enter the cavity when the gate is open, yet the complexes are stabilized when the gate is closed. Guests **B22**−**B29** are predicted to form stable complexes with **2** at higher temperatures, although none have been observed to date. Even with the gate open, the barriers to formation are high.

For all uncomplexed aromatic guests (**B1**−**B21**), our calculated results suggested that these complexes are formed readily in solution. However, the decomplexation processes of these complexes are very easy and thus these complexes are not isolable during purification. Constrictive binding is ineffective because the molecules can get through closed gates. This result is also supported by the comparison of the binding abilities of **2** and **4** toward xylene and dimethoxybenzene guests.[35] Aromatic guests **A10** and **A11** form relatively stable complexes because of their relatively high decomplexation energy barriers and the need for gate-opening for decomplexation.

Acknowledgment. We are grateful to the National Institutes of Health for financial support of this research and to Professor Donald J. Cram, Dr. Young-Seok Byun, Dr. Emily Maverick, Dr. Carolyn B. Knobler, Amy E. Keating, and Dr. Kensuke Nakamura for helpful discussions and unpublished results.

JA9535423